Numerical Simulation of Piezo-Hall Effects in n-Doped Silicon Magnetic Sensors

W. Allegretto, A. Nathan[†], and T. Manku[†]

Department of Mathematics, University of Alberta
Edmonton, Alberta, T6G 2G7, CANADA
[†]Electrical and Computer Engineering, University of Waterloo
Waterloo, Ontario, N2L 3G1, CANADA

Abstract

The output response of n-type Hall sensors are presented for various device (or current flow) orientations in the presence of both stress and magnetic field. The resulting distributions of potential and terminal characteristics are based on a numerical solution of the piezo-Hall transport equation where the conductivity and Hall coefficient are tensors.

1. Introduction

The encapsulation of magnetic sensors induces significant mechanical stresses (due to the piezoresistance effect [1]) affecting accuracy and long term stability of the output response. The stress on the device induces an offset which is highly undesireable when detecting low frequency fields since the offset voltage (or current) and the useful magnetic output signal cannot be distinguished. In addition to the piezoresistance effect, the effects of stress coupled with the magnetic field can potentially affect the magnetic response of Hall devices due to the piezo-Hall effect, which describes the stress-induced modulation of the Hall coefficient [2].

In this paper, we present simulation results of the stress-dependent magnetic response in n-type Hall and split-electrode geometries (Fig. 1) for various device (or current flow) orientations. Unlike previous analytical approaches which are restricted to certain limiting structures [3], the approach presented here is based on a finite element scheme and hence allows simulation of carrier transport and subsequent device optimization for arbitrary device geometries and structures.

2. Modeling Approach

The magnetic field dependent current density in the presence of homogeneous stress reads

$$\mathbf{J_n} - \sigma_\mathbf{n} \cdot [(\mathbf{R_H} \cdot \mathbf{B}) \times \mathbf{J_n}] = \sigma_\mathbf{n} \cdot \mathbf{E} \tag{1}$$

where, the conductivity $\sigma_\mathbf{n}$ is a symmetric second rank tensor. The resistivity $(\sigma_\mathbf{n}^{-1})$ for not too large stress levels, is linearly related to stress, T via the well known fourth rank tensor of piezoresistance coefficients, viz.,

$$(\Delta\rho)_{ij}/\rho_0 = \Sigma_{k,l} \; \pi_{ijkl} T_{kl}. \tag{2}$$

The Hall coefficient tensor, $\mathbf{R_H}$ carries a similar form but it is related to the fourth rank tensor of piezo-Hall coefficents,

$$(\Delta R_H)_{ij}/R_{Ho} = \Sigma_{k,l} \; P_{ijkl} T_{kl}, \tag{3}$$

values of which have been measured only recently [4]. In the absence of stress, the

conductivity and Hall coefficient become scalars, and the original form of the equation in terms of the electron Hall mobility, μ_{Hn} (= $|\sigma_n R_H|$) is recovered [5].

We transform eqn. (1) from the cubic crystallographic axes to the Cartesian system of arbitrary orientation. The transformation of vectors $\mathbf{J_n}$ and $\mathbf{E}$ lead to $\mathbf{J_n}' = \alpha \mathbf{J_n}$ and $\mathbf{E}'$ = $\alpha \mathbf{E}$, where α is the transformation matrix expressed in terms of Euler's angles [6]. The reduced form of equation (1) reads

$$\mathbf{J_n}' = \mathbf{A} \cdot \mathbf{E}', \tag{4}$$

where, $\mathbf{A}$ is an asymmetric second rank tensor which contains terms in conductivity ($\sigma_n' = \alpha \sigma_n \alpha^{-1}$) and Hall coefficient ($\mathbf{R_H}' = \alpha \mathbf{R_H} \alpha^{-1}$) both being functions of stress ($\mathbf{X}$ = $\alpha T \alpha^{-1}$), and the magnetic field ($\mathbf{B}' = \alpha \mathbf{B}$). The matrix becomes skew symmetric in the absence of stress and becomes symmetric in the absence of both stress and magnetic field.

Consider a two-dimensional system with the orientations of current, magnetic field, and uniaxial stress as depicted in Fig. 2. Assuming negligible generation or recombination in the device, the divergence of the current density in (4) under steady state conditions can be cast into the following form:

$$\Sigma_{i,j=1,2} \quad D_i \left(a_{ij} D_j \, \psi \right) = 0 \tag{5}$$

where $D_1 = \partial/\partial x$, $D_2 = \partial/\partial y$, and the entries a_{ij}, which carry a cumbersome form, will not be shown for convenience. The boundary conditions for (5) consist of Dirichlet conditions (prescribed by the applied potential) at the current electrodes and the Neumann condition at insulating boundaries, $\mathbf{J_n}' \cdot \mathbf{n} = 0$, where $\mathbf{n}$ denotes the outward normal vector. We observe that the latter is a natural condition associated with (5) and is influenced by both the stress and the magnetic field. At the Hall probe regions in the Hall geometry, we impose the condition, $\int_{probe} (\mathbf{J_n}' \cdot \mathbf{n}) \, d(probe) = 0$, since we are only interested in the open circuit Hall voltage. Equation (5), together with the boundary conditions, is numerically solved based on a standard Galerkin finite element discretization procedure, using an adaptively generated grid. Since the conditions at the insulating boundaries are natural to (5), the discretization procedure is simplified. The numerical scheme employed here is based along the lines discussed in [5].

3. Results and Discussion

The samples considered in the analysis are n-type of <100> and <110> crystallographic orientations with doping concentrations in the range 10^{14} - 10^{16} cm^{-3}. The values of piezo-Hall coefficients used in the computations are based on the measurement data reported in [4]. In practical device structures, the stress on the device is induced primarily by encapsulation (or packaging), and arises mainly due to the difference in thermal expansion coefficients between the silicon die and the epoxy employed in the bonding process. To obtain practical estimates of the stress on the die surface, the general purpose finite element software package ANSYS [7] was used. The simulated stress distribution on the die surface is shown in Fig. 2.

Using a stress value, $X = 10^8$ dyne/cm^2, the output response for both (100) and (110) Hall and split-drain devices is computed as a function of device orientation. Here, we rotate the current density, J about a given direction by an angle ψ, keeping the directions of magnetic field, B and stress, X fixed (Fig. 3). For example, with no rotation, $\psi = 0°$; J || X || <010>, B || <100> for (100) devices, and J || X || <001>, B || <110> for the (110) counterparts.

The output voltage for the Hall geometry, calculated at B = 0 and at B = 100 mT is shown

in Fig. 4 for $J = 2 \times 10^4$ A/cm^2. Here, we see that the offset is zero when the device is oriented such that the current flow is parallel or transverse to the uniaxial stress. Any variation from these directions gives rise to an offset, and in particular, at angles 45° from these directions, the offset is seen to be a maximum. As expected, stresses acting on the <100> sample result in higher output voltages compared with the <110> orientation due to its relatively larger piezoresistance coefficient. Although not shown, the same behaviour is noted for the output current $(I_1 - I_2)$ of the split-electrode device geometry.

No significant nonlinear coupling between the stress and the magnetic field was noted at fields, B ≤1 Tesla. This can be noted from the Hall voltage response in Fig. 4. The output Hall voltage at 100 mT field is simply the zero field response shifted by an amount which corresponds to the "unstressed" Hall voltage. At relatively larger fields (B = 2 Tesla), a very weak (hardly noticeable) interaction can be observed in the potential distribution (see Fig. 5). This coupling, however, is not significant for practical values of field strengths.

Conclusions

In this paper, we have presented two-dimensional numerical solutions to the piezo-Hall current density equation which accounts for the effects of stress on galvanomagnetic carrier transport. The interaction between the stress and magnetic field was found to be very weak and evident only at large field strengths.

References

[1]   C. S. Smith, Phys. Rev. **94** (1954) 42.
[2]   R. W. Keyes, Solid State Physics **11** (1960) 149.
[3]   A. Nathan, T. Manku, Appl. Phys. Lett. **62**, No. 23 (1993) in press.
[4]   B. Hälg, *J. Appl. Phys.* **64** (1990) 276-282.
[5]   W. Allegretto, A. Nathan, H. Baltes, *IEEE Trans. CAD* **10** (1991) 501-511.
[6]   Y. Kanda, IEEE Trans. Electron Devices ED-29 (1984) 64.
[7]   User's Manual, ANSYS Engineering Analysis System, Houston: Swanson Analysis Systems Incorporated.
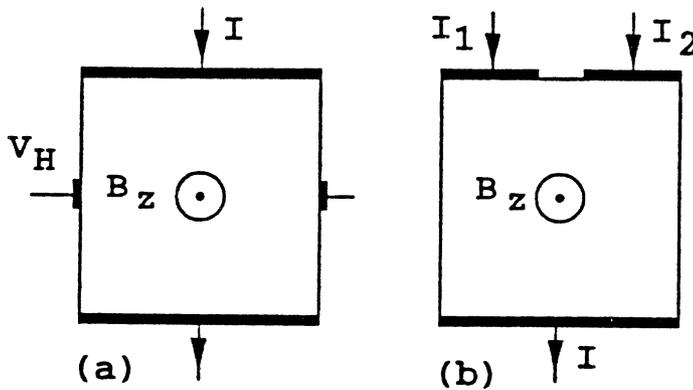
Fig. 1 (a) Hall and (b) split-electrode devices considered in analysis.
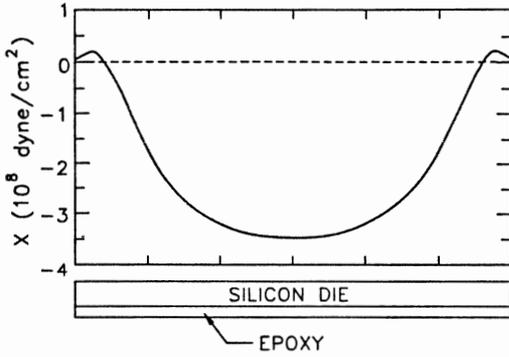
Fig. 2 Simulated stress distribution on die surface.
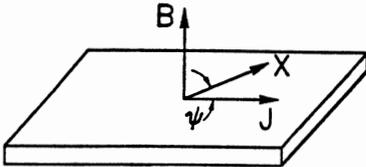
Fig. 3 Orientations of current density, magnetic field, and uniaxial stress.
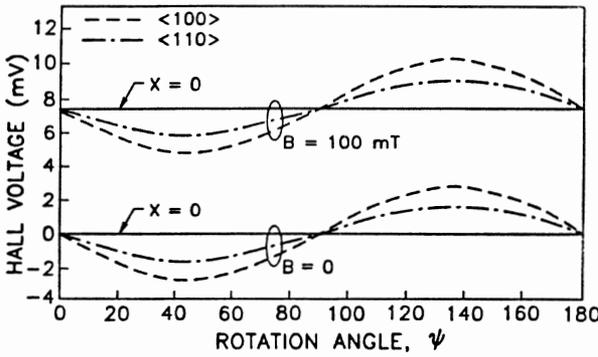
Fig. 4 Output response of (100) and (110) Hall geometries as a function of device orientation under uniaxial stress of 10^8 dynes/cm^2.
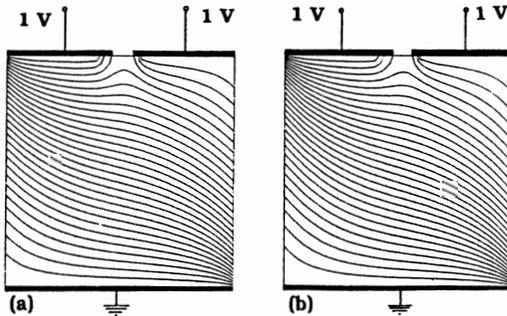
Fig. 5 Equipotential lines in the (100) split-electrode under 10^8 dynes/cm^2 for (a) B = 0 T and (b) B = 2 T. The orientations are B ∥ <100>, X ∥ <010>, and J ∥ <011>. The rotation angle is $\psi = 45°$.